Electrochemical co-deposition of Erbium and Ytterbium in molten LiF-CaF2: An original way for lanthanides extraction on inert electrode

Laurent Massot, H. Meskine, M. Gibilaro, P. Chamelot

Version of Record: https://www.sciencedirect.com/science/article/pii/S0022113922000306
Manuscript_4a9a1ded825072d1a00b13a3b97714df

Electrochemical co-deposition of Erbium and Ytterbium in molten LiF-CaF_2: an original way for lanthanides extraction on inert electrode

L. Massot*, H. Meskine, M. Gibilaro, P. Chamelot

Laboratoire de Génie Chimique; Université de Toulouse; CNRS; INPT; UPS;

Toulouse, France

* Corresponding author

laurent.massot@univ-tlse3.fr

tel: +33 5 61 55 81 94

fax: +33 5 61 55 61 39

Abstract

Electrochemical study of Er(III)/Er and Yb(III)/Yb systems was independently investigated in molten LiF-CaF_2 on inert electrode at 840°C using cyclic voltammetry and square wave voltammetry. Experimental results showed that two different behaviours were observed: Er(III) was reduced into metal in a one-step and diffusion controlled process and Yb(III) was first reduced into Yb(II) then into Yb. The electrochemical study of LiF-CaF_2 containing both Er(III) and Yb(III) on inert Mo electrode highlighted a co-deposition of Er and Yb leading to Er-Yb surface alloys formation. Alloys formation was evidenced using open-circuit chronopotentiometry and SEM-EDS. Finally, co-extraction of Er and Yb from molten salt was carried out by electrolysis with high extraction efficiency (> 99.5 %). These results pave the way to the Lanthanides extraction without involving cathode material nor another ion as for reactive electrodeposition.

Keywords

Electrochemical co-reduction, Erbium, Ytterbium, molten fluorides, lanthanides co-extraction

1/ Introduction

Pyrochemical processes are mainly envisaged for the reprocessing of nuclear spent fuels in the frame of a sustainable development of nuclear energy production [1,2]. The interest of pyroprocesses is based on the properties of the molten salt phase: high radiation and thermal resistance and relative high transparency to neutrons. Pyrometallurgical processes are also attractive for the dissolution of fuels or inert matrices, which are very difficult or impossible in aqueous media. A key-step for spent nuclear fuel reprocessing is the separation of actinides (Ans) from lanthanides (Lns), due to their similar properties. Electrochemical processes in molten salts are very promising by using precipitation with oxide ions [3], electrodeposition

[4,5] or reductive extraction [6]. The ultimate step is to extract Lns from the solvent to recycle it. In the last twenty years, the study on the electrodeposition process in molten salts have attracted great interest. Two ways are possible, depending on the Ln reduction potential E_{Ln}:

- if the Lns ions can be reduced into metal at a potential significantly higher than the solvent cations reduction one, then Lns can be electrodeposited on an inert cathode;
- if the Lns ions reduction into metal cannot be observed on a voltammogram (reduction occurring at a lower potential than the cathodic electrochemical window), UnderPotential Deposition (UPD) has to be implemented.

UPD is obtained by reactive electrodeposition with the cathode substrate or by co-reduction with another species (AlF_3). It has been successfully carried out in our laboratory to extract NdF_3, GdF_3, CeF_3, EuF_3 and SmF_3 [7-11] from molten LiF-CaF_2 in the 840-950°C temperature range with an extraction efficiency higher than 99%.

These techniques lead to Ln-Ni, Cu, Al alloys, and the major drawback of these methodologies is that Lns are not deposited into pure metal form, leading to the consumption of the cathode material, or Al ions content in the bath. An additional step is also needed to recover pure Ln metals from alloys.

This article proposes an original way to extract Lns from a molten fluoride salt (LiF-CaF_2) without involving reactive species. The methodology proposed consists in the co-reduction of two lanthanides which have different reduction pathways (one or two reduction steps) on inert electrode. Erbium (Er) and Ytterbium (Yb) were selected to demonstrate the feasibility of this approach. Studies in molten chloride media are available and are resumed below:

- Er(III)/Er system:

Castrillejo *et al*. [12], Cao *et al*. [13] and Tang *et al*. [14] studied the electrochemical behaviour of Er(III) into molten LiCl-KCl on inert electrode and the obtained results showed that Er(III) reduction into Er is a one-step process, exchanging 3 electrons and limited by diffusion into the solution. Reactive electrodeposition of Er(III) has also been investigated by Sun Yi *et al*. with the formation of Al-Li-Er alloys into molten LiCl-KCl-$AlCl_3$-Er_2O_3 [15] and Wang *et al*. who prepared Er-Mg alloys on Mg electrodes [16].

- Yb(III)/Yb system:

Smolenski *et al*. [17], Novoselova *et al*. [18] and Castrillejo *et al*. [19] investigated Yb(III) electrochemical behaviour on inert W electrode into molten LiCl-KCl, NaCl-KCl, CsCl and NaCl-KCl-CsCl in the 450 – 800 °C temperature range. All the studies showed that Yb(III) was reduced into Yb(II) in a one-step process limited by diffusion into the solution. Castrillejo *et al.* [19] also evidenced the formation of Al-Yb alloys by UPD on Al electrode, proving that the reduction of Yb(II) into Yb occurred at a potential lower than solvent reduction.

As no publication can be found on the electrochemical behaviour of Er(III) and Yb(III) in molten fluorides, the first part of the present article is dedicated to the electrochemical behaviour of ErF_3 and YbF_3 into molten LiF-CaF_2 on inert Mo electrode. Then the co-reduction of Er(III) and Yb(III) on inert electrode is examined by using cyclic voltammetry, square wave voltammetry and open-circuit chronopotentiometry in the 840-930°C temperature range. The final part concerns the simultaneous extraction of both elements and the extraction efficiency has been determined.

2/ Experimental

The cell was made of a vitreous carbon crucible placed in a refractory steel cylindrical vessel closed by a lid cooled by circulating water and protected against fluoride vapours by a graphite liner on its inner part. Experiments were performed under argon atmosphere (99.999%). The operating temperatures were measured using a thermocouple placed into the molten salt. The solvent consisted of a LiF-CaF_2 (Merck 99.99%) mixture (eutectic composition: 79.5/20.5 molar ratio), initially dehydrated by heating under vacuum to its melting point.

Erbium and Ytterbium ions were introduced in the form of ErF_3 and YbF_3 powder (Merck 99.99%) respectively.

The working and auxiliary electrodes were a Molybdenum wire (Goodfellow 99.99%, 1mm diameter) and a vitreous carbon rod (5 mm diameter) respectively. The working electrode surface area was accurately determined by measuring the immersion depth when the electrode was taken out of the furnace after each experiment.

A platinum wire (Alfa Aesar 99.95%, 1mm diameter) immersed in the electrolyte was used as quasi-reference electrode $Pt/PtO_x/O^{2-}$. In order to compare the electrochemical systems, whatever the oxide ions content, all the potentials were referred to the equilibrium potential of LiF/Li system, acting as intern reference. This equilibrium potential was firstly measured using cyclic voltammetry on Mo electrode and then was subtracted to the potentials.

The electrochemical study and the electrolyses were performed by cyclic and square wave voltammetries and open-circuit chronopotentiometry with an Autolab PGSTAT 302N potentiostat / galvanostat controlled with NOVA 2.1 software.

The electrodes were observed and characterized after electrolysis by Scanning Electron Microscopy coupled to Energy Dispersive Spectroscopy probe (Phenom XL SEM-EDS).

Inductively coupled plasma – atomic emission spectroscopy (ICP – AES Horiba Ultima 2) was used for Er(III) and Yb(III) content determination after sampling of the melt.

3/ Results and discussion

3-1/ Electrochemical study of $LiF-CaF_2-ErF_3$ and $LiF-CaF_2-YbF_3$ systems

Cyclic and square wave voltammetries were carried out to investigate the electrochemical behaviour of Er(III) and Yb(III) on Mo electrode in the $LiF-CaF_2-ErF_3$ and $LiF-CaF_2-YbF_3$ systems at 840°C.

3-1-1/ Electrochemical behaviour determination

Figures 1a and 1b present typical cyclic voltammograms plotted on Mo electrode at 840°C and 100 $mV.s^{-1}$ for $LiF-CaF_2-ErF_3$ (0.139 $mol.kg^{-1}$) and $LiF-CaF_2-YbF_3$ (0.143 $mol.kg^{-1}$) systems respectively. On both voltammograms, it can be observed a single cathodic peak at around 0.07 V vs. LiF/Li for Er(III) and around 0.9 V vs. LiF/Li for Yb(III). For Er(III) system, the cathodic peak is correlated to one reoxidation peak with a stripping shape characteristic of solid phase dissolution, whereas reoxidation peak shape observed for Yb(III) system indicates the formation of soluble compound during cathodic scan.

As presented in the Fig. 1a and Fig. 1b insets, the quasi-reversibility of both systems, characterized by Er(III) and Yb(III) reduction peak potentials independent of the scan rate, is verified. Additional reduction peak was observed at around 0.5V. As this reduction peak was not observed in pure LiF-CaF2, and its current density was very low, this system was attributed to the presence of impurity in the ErF_3 powder.

A linear variation of the cathodic peak current densities as function of molality is presented in Figure 2 for Yb(III) reduction (grey) and Er(III) reduction (black). These relationships are given at 840 °C:

$j_p = -0.26$ [Yb(III)] (1)

$j_p = -3.62$ [Er(III)] (2)

where j_p the peak current density, [Yb(III)] and [Er(III)] the lanthanide molality (mol kg^{-1}). These equations allow the in situ determination of Er(III) and Yb(III) content in the molten medium at 840°C.

In order to determine the number of exchanged electrons involved into their reduction, square wave voltammetry was performed and the voltammograms obtained on Mo electrode at 25Hz for LiF-CaF_2-ErF_3 and LiF-CaF_2-YbF_3 are presented on Fig. 3a and 3b respectively.
These SWV voltammograms highlight one reduction peak at around 0.07 and 0.9 V vs. LiF/Li for Er(III) and Yb(III) systems respectively, as observed on the CV voltammograms of Fig. 1a and 1b. As the linearity of differential peak current density versus the square root of the frequency is verified for both systems (Fig 3a and 3b insets), the SWV voltammograms were deconvoluted using the methodology previously published in our laboratory [20]. This signal treatment allows the number of exchanged electrons to be determined using equation (3) [21]:

$$w_{1/2} = 3.52\frac{RT}{nF} \quad (3)$$

where n is the number of exchanged electrons, F the Faraday constant (96500 C), T the absolute temperature in K and R the ideal gas constant (J mol^{-1} K^{-1}).

The obtained number of exchanged electrons are 3±0.1 for Er(III) reduction and 1±0.1 for Yb(III) reduction.

With these results, the following reactions can thus be assumed, similarly to molten chloride media:

$Er(III) + 3\ e^- = Er$ (4)

$Yb(III) + e^- = Yb(II)$ (5)

It can be noted that Yb(II) reduction into Yb metal is not observed in the electrochemical window, meaning that the extraction of Yb from molten LiF-CaF_2 in a pure metallic form is not possible, as previously observed for Eu and Sm in molten LiF-CaF_2 [22;23].

3-1-2/ Diffusion coefficient

Er(III) and Yb(III) reduction peak current densities variations versus the square root of the CV scan rate are presented in the Fig. 1a and Fig. 1b insets. Berzins Delahaye and Randles Sevcik relationships, valid for reversible and diffusion-controlled soluble/insoluble (Er(III)/Er system) and soluble/soluble (Yb(III)/Yb(II) system) systems respectively are given in eqs. (5) and (6) [21]:

$$\boldsymbol{I_p} = -0.61\mathrm{nFSc_0}\left(\frac{\mathrm{nF}}{\mathrm{RT}}\right)^{1/2}\boldsymbol{D^{1/2}v^{1/2}} \quad (6)$$

$$\boldsymbol{I_p} = -0.44\mathrm{nFSc_0}\left(\frac{\mathrm{nF}}{\mathrm{RT}}\right)^{1/2}\boldsymbol{D^{1/2}v^{1/2}} \quad (7)$$

where S the electrode surface area in cm^2, D the diffusion coefficient in $cm^2\ s^{-1}$, c_0 the solute concentration in mol cm^{-3} and v the potential scan rate in V s^{-1}.

The slope of the linear equations at 840°C (insets of Figs. 1a and 1b), proving that reactions are controlled by Ln(III) diffusion into the solution, are:

- For Er(III) reduction: $\frac{\mathbf{i_p}}{\mathbf{v^{1/2}}} = \mathbf{-0.832\ A\ s^{1/2}V^{-1/2}cm^{-2}}$ (8)
- For Yb(III) reduction: $\frac{\mathbf{i_p}}{\mathbf{v^{1/2}}} = \mathbf{-0.209\ A\ s^{1/2}V^{-1/2}cm^{-2}}$ (9)

Diffusion coefficients are determined from eqs. (8) and (9):

$$D_{Er(III)} = (9.1 \pm 0.2)x10^{-6}\ cm^2s^{-1} \quad (10)$$

$$D_{Yb(III)} = (2.57 \pm 0.02)x10^{-5}\ cm^2s^{-1} \quad (11)$$

All these experiments were carried out in the 840 - 930 °C temperature range and the obtained values, plotted in Fig. 4, show that the variation of diffusion coefficient with the temperature obeys Arrhenius' like law expressed as:

$$\ln(D_{Er(III)}) = -17.32 - \frac{3891.1}{T} \quad (12)$$

$$\ln(D_{Yb(III)}) = -16.79 - \frac{3328.9}{T} \quad (13)$$

where $D_{Er(III)}$ and $D_{Yb(III)}$ are in $m^2\ s^{-1}$ and T in K.

3-2/ Electrochemical study of $LiF-CaF_2-ErF_3-YbF_3$ system

The electrochemical behaviour of each Ln ions was thus determined in molten fluoride salt and their mixing in the same solution is presented in this part.

Experiments were carried out on Mo electrode at 840°C using cyclic voltammetry and square wave voltammetry, and the obtained plots are presented in Fig. 5a and Fig. 5b respectively. The observations on both CV and SWV voltammograms are similar:

- two reduction peaks are observed at around 0.08 and 0.9 V vs. Li(I)/Li. In agreement with the results presented above, these two peaks are attributed to Er(III)/Er and Yb(III)/Yb(II) systems respectively,
- in between these two potentials, a significant reduction current density is evidenced. As no signal was observed at these potentials when only one species was present in the solution, this new cathodic current can be attributed to the Er-Yb co-reduction, as previously observed in our Laboratory for Al-Lns co-reduction [9].

Moreover, this cathodic current is observed for potentials lower than the peak potential of Yb(III) reduction into Yb(II), indicating a co-reduction between Er(III) and Yb(II) species. The following overall reaction can be written:

$$x\ Er(III) + y\ Yb(II) + (3x + 2y)\ e^- = Er_xYb_y \qquad (14)$$

In order to evidence alloys formation and to confirm Er and Yb co-deposition on inert Mo electrode, open-circuit potentiometry was performed. After a short cathodic polarization at -400 mA cm^{-2} during 15 s (see Figure 6), some potential plateaus can be observed:

- two plateaus at around 0.08 and 1.4 V vs. Li(I)/Li, corresponding to Er(III)/Er and Yb(III)/Yb(II) potential respectively,
- three supplementary ones, at around 0.3, 0.4 and 0.8 V vs. Li(I)/Li. In agreement with CV and SWV results, these plateaus can be attributed to Er-Yb co-reduction leading to the formation of alloys or defined compounds, proving the Er and Yb simultaneous co-deposition on inert Mo cathode. The number of plateaux should correspond to the number of compounds produced.

Electrolyses were realized on Mo electrodes in order to observe and characterize the produced Er-Yb compounds using SEM-EDS, where the imposed potentials correspond to the potential plateaus observed in Fig.6. The micrographs and SEM analyses of Mo electrodes surfaces after polarisation during 1800s at 840°C are gathered on Fig. 7a (E=0.8 V), 7b (E=0.4 V) and 7c (E=0.3 V).

It can be noted that Er-Yb metallic compounds are detected on each micrography. Different compositions are observed ($ErYb_2$, Er_2Yb_3 and Er_2Yb) and the higher the potential is, the richer in Yb the compound is. These results clearly prove that Er-Yb electrochemical co-deposition occurred. Moreover, deposits seem to be adherent enough to envisage Er and Yb extraction from the molten solution by potentiostatic electrolyses.

3-3/ Electrochemical extraction of Er and Yb

The erbium and ytterbium co-extraction from molten LiF-CaF_2 was realised by potenstiostatic electrolyses on Mo plate at 840°C with the following methodology:

- the electrolysis potential was chosen equal to 0.4 V vs. Li(I)/Li,
- several electrolyses of relatively short durations were performed and after eah electrolysis, cyclic voltammogram was plotted on Mo electrode and the cathode was renewed after each measurement,
- the progress of the extraction can classically be followed by *in situ* measurements of residual species content in the bath, using cyclic voltammetry and the calibration relationships (eqs. 1 and 2). Er(III) reduction peak on Mo electrode was selected due to its lower potential and higher intensity than Yb(III) ones. The extraction yield was thus expressed as the ratio of Er(III) reduction peak current density measured after electrolysis and the initial one,
- a normalized time t*, defined in refs [10, 23], was applied in the present work:

$$t^* = t\,\frac{S_{el}}{V_{sol}} \qquad (15)$$

where t is the time (h), S_{el} is the cathode surface area (cm^2), V_{sol} is the volume of the solution (cm^3) and t* is the normalized time (h cm^{-1}).

Typical square wave voltammograms are presented in Figure 8 where a significant decrease of the current density can be observed during the extraction process, correlated to the decrease of Er(III) and Yb(III) ions concentration in the bath. As showed in Figure 9, representing the extraction progress versus the normalized time, the concentration decreased more quickly at the beginning of the electrolysis.

The maximum progress was reached after 4 h cm^{-1} of electrolysis. At the end of experiments, the cathodic current density value was approaching zero on the square wave voltammogram and the extraction efficiency was calculated with ICP analysis of Er and Yb in the salt. The obtained value is equal to 99.5 % for Er(III) and Yb(III), showing a quasi-total extraction of both Ln from the salt on an inert electrode.

4/ Conclusion

In the frame of molten fluoride solvent recycling in spent nuclear fuel pyrochemical reprocessing, lanthanides extraction was performed by co-reduction on inert metallic substrate and thus, the solvent could be recycled. To make this co-deposition possible, at least two lanthanide species are initially needed: one Ln ion which is reduced into metal in a one-step process and another one with a two-step reduction mechanism, as in this work.

The Er(III) and Yb(III) electrochemical behaviour was investigated in the LiF-CaF_2-ErF_3 and LiF-CaF_2-YbF_3 systems on inert electrode. This study evidenced the two different electrochemical reduction pathways, as mentioned above.

Diffusion coefficients were also determined in the 840-930°C temperature range and the results show a dependence of ln D with the inverse of the temperature.

Electrochemical experiments in the LiF-CaF_2-ErF_3-YbF_3 system evidenced the co-reduction of both ions leading to Er-Yb alloys formation on Mo electrode. The obtained alloys are $ErYb_2$, Er_2Yb_3 and Er_2Yb.

Potentiostatic electrolyses were carried out on Mo plate and a complete Ln extraction was achieved (99.5% for both ions) after a normalized duration of 4 h cm^{-1}.

As a perspective, the methodology can be applied to others lanthanides elements which are known to be reduced into metal in a two-step process in molten fluorides: samarium and europium.

References

[1] J.P. Ackerman, Chemical basis for pyrochemical reprocessing of nuclear fuel, Ind. Eng. Chem. Res. 30(1) (1991) 141-145

[2] T. Inoue, L. Koch, Development of pyroprocessing and its future direction, Nucl. Eng. Technol. 40 (2008) 183-190

[3] D. Lambertin, S. Sanchez, G. Picard, J. Lacquement, Temperature dependence and effect of oxide anion on the americium chemistry in the molten LiCl-KCl eutectic, Radiochim. Acta 91 (2003) 449-452

[4] M. Iizuka, T. Koyama, N. Kondo, R. Fujita, H. Tanaka, Actinides Recovery from Molten Salt/Liquid Melt System by Elecrochemical Methods, J. Nucl. Mater. 247 (1997) 183-190

[5] P. Chamelot, L. Massot, C. Hamel, C. Nourry, P. Taxil, Feasibility of the electrochemical separation of An, Ln, solvent in molten fluorides, J. Nucl. Mater. 360 (2007) pp. 64-74.

[6] L. Rault, M. Heusch, M. Allibert, F. Lemort, X. Deschanel, R. Boen, Test of Actinide-Lanthanide Separation in an Aluminum-Based Pyrochemical System, Nucl. Technol. 139 (2002) 167-174

[7] M. Gibilaro, L. Massot, P. Chamelot, P. Taxil, Study of neodymium extraction in molten fluorides by electrochemical co-reduction with aluminium, J. Nucl. Mater. 382 (2008) pp. 39-45

[8] P. Taxil, L. Massot, C. Nourry, M. Gibilaro, P. Chamelot, L. Cassayre, Lanthanides extraction processes in molten fluoride media. Application to nuclear spent fuel reprocessing, J. Fluor. Chem. 130 (2009) pp. 94-101

[9] M. Gibilaro, L. Massot, P. Chamelot, P. Taxil, Co-reduction of aluminium and lanthanide ions in molten fluorides: application to cerium and samarium extraction from nuclear waste, Electrochim. Acta 54 (2009) pp. 5300-5306

[10] C. Nourry, L. Massot, P. Chamelot, P. Taxil, Neodymium and gadolinium extraction from molten fluorides by reduction on a reactive electrode, J. App. Electrochem. 39 (2009) pp. 2359-2367

[11] M. Gibilaro, L. Massot, P. Chamelot, L. Cassayre, P. Taxil, Electrochemical extraction of europium from molten fluoride media, Electrochim. Acta 55 (2009) pp. 281-287.

[12] Y. Castrillejo, M.R. Bermejo, E. Barrado, A.M. Martınez, Electrochemical behaviour of erbium in the eutectic LiCl–KCl at W and Al electrodes, Electrochim. Acta 51 (2006) 1941–1951

[13] P. Cao, M. Zhang, W. Han, Y. Yan, S. Wei, Electrochemical behaviour of erbium and preparation of Mg-Li-Er alloys by codeposition, J. Rare Earths 29 (2011) 763-767

[14] H. Tang, B. Pesic, Electrochemistry of $ErCl_3$ and morphology of erbium electrodeposits produced on Mo substrate in early stages of electrocrystallization from LiCl–KCl molten salts Electrochim. Acta 133 (2014) 224-232

[15] Y. Sun, M. Zhang, W. Han, Y. Yan, Y. Yang, Y. Sun, Electrochemical behaviour and codeposition of Al-Li-Er alloys in LiCl-KCl-$AlCl_3$-Er_2O_3 melts, J. Rare Earths 31 (2013) 192-197

[16] Y. Wang, M. Li, W. Han, M. Zhang, Y. Yang, Y. Sun, Y. Zhao, Y. Yan, Electrochemical extraction and separation of praseodymium and erbium on reactive magnesium electrode in molten salts, J. Solid State Electrochem. 19 (2015) 3629-3638

[17] V. Smolenski, A. Novoselova, A. Osipenko, C. Caravaca, G. de Cordoba, Electrochemistry of ytterbium (III) in molten alkali metal chlorides, Electrochim. Acta 54 (2008) 382–387

[18] A. Novoselova, V. Smolenski, Thermodynamic properties of thulium and ytterbium in fused NaCl–KCl–CsCl eutectic, J. Chem. Thermodynamics 43 (2011) 1063–1067

[19] Y. Castrillejo, P. Fernandez, J. Medina, M. Vega, E. Barrado, Chemical and Electrochemical Extraction of Ytterbium from Molten Chlorides in Pyrochemical Processes, Electroanalysis 23 (2011) 222 – 236

[20] C. Nourry, L. Massot, P. Chamelot, P. Taxil, Data acquisition in thermodynamic and electrochemical reduction in a Gd(III)/Gd system in LiF–CaF_2 media, Electrochimica Acta 53 (2008) 2650–2655.

[21] A. J. Bard, R. L. Faulkner, Electrochemistry: principles, methods and applications, Wiley Ed., New York, 1980.

[22] L. Massot, P. Chamelot, P. Taxil, Cathodic behaviour of samarium(III) in LiF-CaF2 media on molybdenum and nickel electrodes, Electrochim. Acta 50 (2005) 5510-5517.

[23] L. Massot, P. Chamelot, L. Cassayre, P. Taxil, Electrochemical study of the Eu(III)/Eu(II) system in molten fluoride media, Electrochim. Acta 54 (2009) 6361-6366.

Legend of figures

Figure 1a:

Cyclic voltammograms of LiF-CaF_2-ErF_3 (0.139 mol kg^{-1}) system at 100 mV s^{-1} and T = 840°C. Inset: Variations of reduction peak current density (left axis) and reduction peak potential (right axis) versus the square root of scan rate on Mo in LiF-CaF_2-ErF_3 at 840°C

Figure 1b:

Cyclic voltammograms of LiF-CaF_2-YbF_3 (0.143 mol kg^{-1}) system at 100 mV s^{-1} and T = 840°C. Inset: Variations of reduction peak current density (left axis) and reduction peak potential (right axis) versus the square root of scan rate on Mo in LiF-CaF_2-YbF_3 at 840°C

Figure 2:

Linear relationship between YbF_3 (black) and ErF_3 (grey) molality and reduction peak current density on Mo at 100 mV s^{-1} in LiF-CaF_2 at 840 °C

Figure 3a:

Square wave voltammogram of LiF-CaF_2-ErF_3 (0.139 mol kg^{-1}) at 25 Hz and T = 840°C. Inset: Variation of SWV reduction peak current density versus square root of frequency on Mo in LiF-CaF_2-ErF_3 at 840°C

Figure 3b:

Square wave voltammograms of LiF-CaF_2-YbF_3 (0.143 mol kg^{-1}) at 25 Hz and T = 840°C. Inset: Variation of SWV reduction peak current density versus square root of frequency on Mo in LiF-CaF_2-YbF_3 at 840°C

Figure 4:

Linear relationships between ln(D) and the inverse of absolute temperature in LiF-CaF_2-YbF_3 (black) and LiF-CaF_2-ErF_3 (grey) on Mo electrode

Figure 5a:

Cyclic voltammogram of LiF-CaF_2-ErF_3 (0.139 mol kg^{-1}) -YbF_3 (0.143 mol kg^{-1}) system on Mo at 100 mV s^{-1} at 840°C

Figure 5b:

SWV voltammogram of LiF-CaF_2-ErF_3 (0.139 mol kg^{-1}) -YbF_3 (0.143 mol kg^{-1}) system on Mo at 25 Hz and 840°C

Figure 6:

Open-circuit chronopotentiogram of LiF-CaF_2-ErF_3-YbF_3 system after polarization at -400 mA cm^{-2} during 15 s at 840 °C

Figures 7a, b and c:

SEM micrographs of Mo electrodes after electrolysis at (a) 0.8 V vs. Li(I)/Li; (b) 0.4 V vs. Li(I)/Li and (c) 0.3 V vs. Li(I)/Li during 1800 s at 840°C.

Figure 8:

Variation of the square wave voltammograms of the LiF-CaF_2-ErF_3-YbF_3 system at 100 mV s^{-1} and 840°C for three electrolysis times on Mo plate.

Figure 9:

Variation of the extraction progress at 840°C versus normalized time.

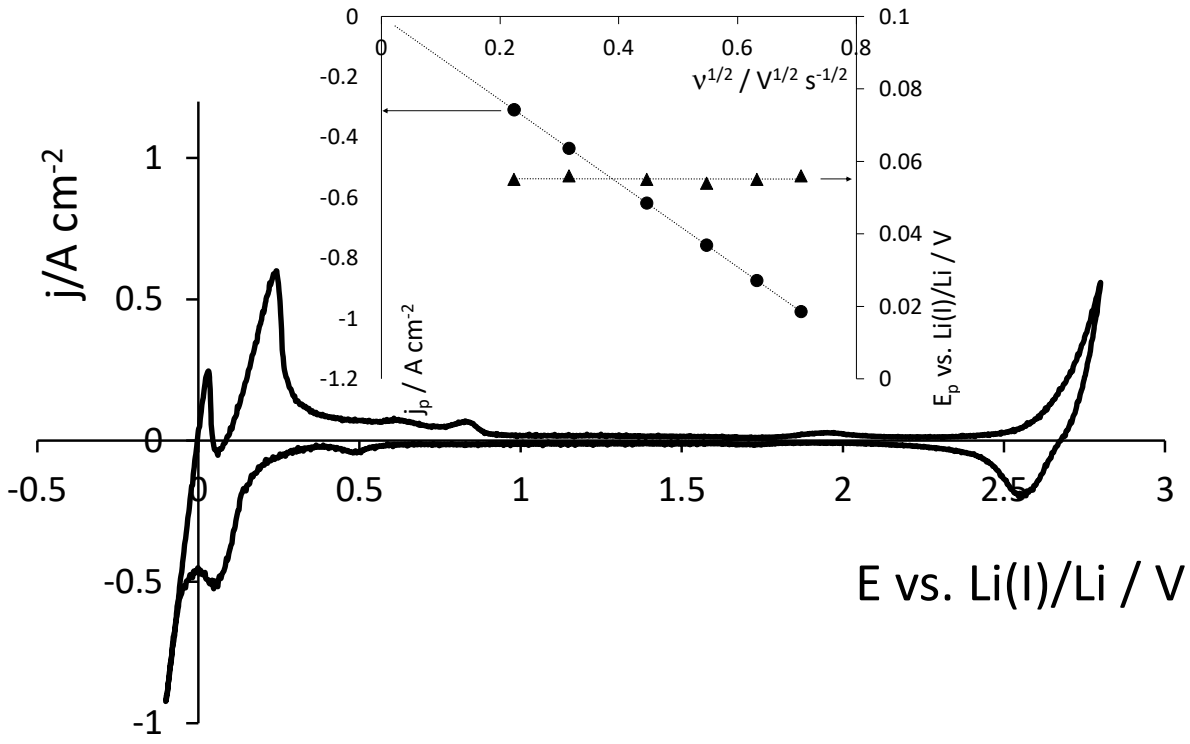

Figure 1a

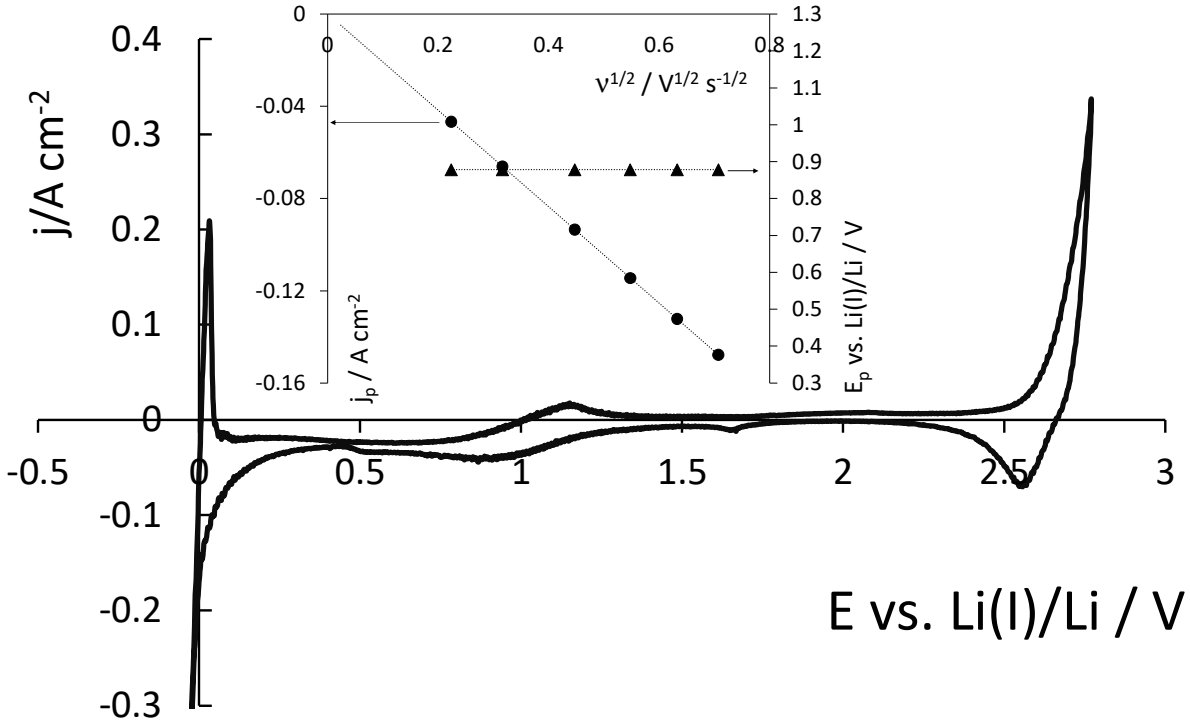

Figure 1b

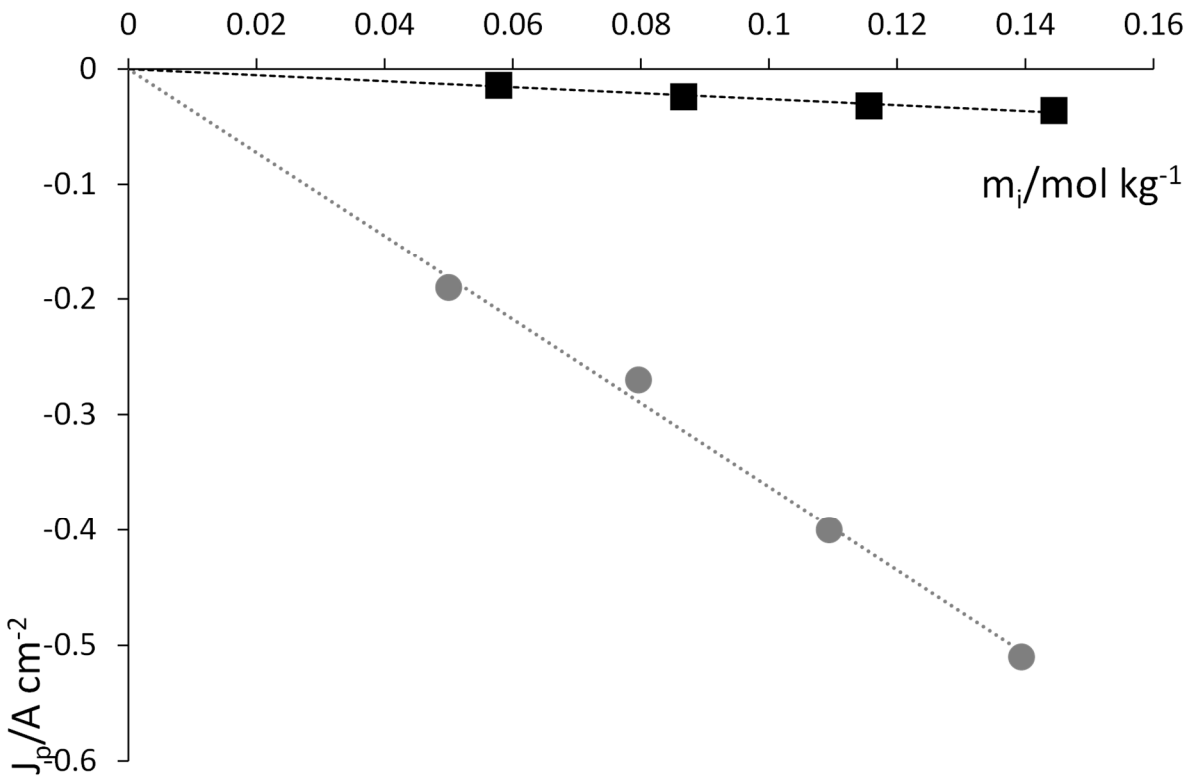

Figure 2

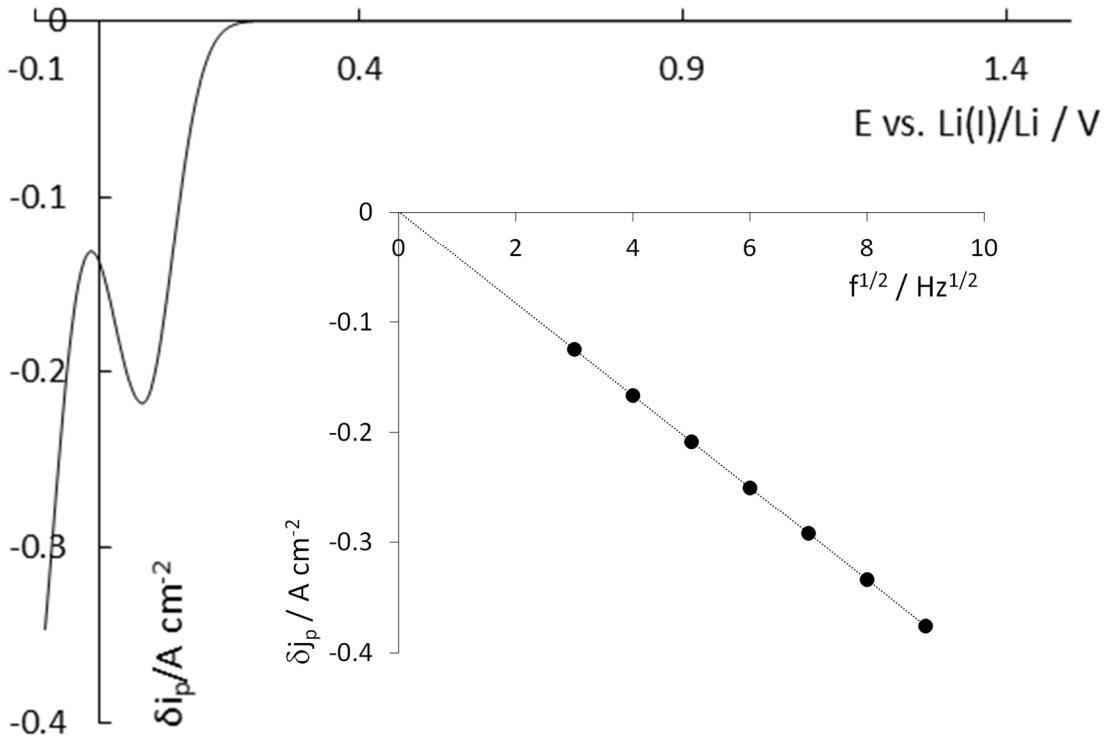

Figure 3a

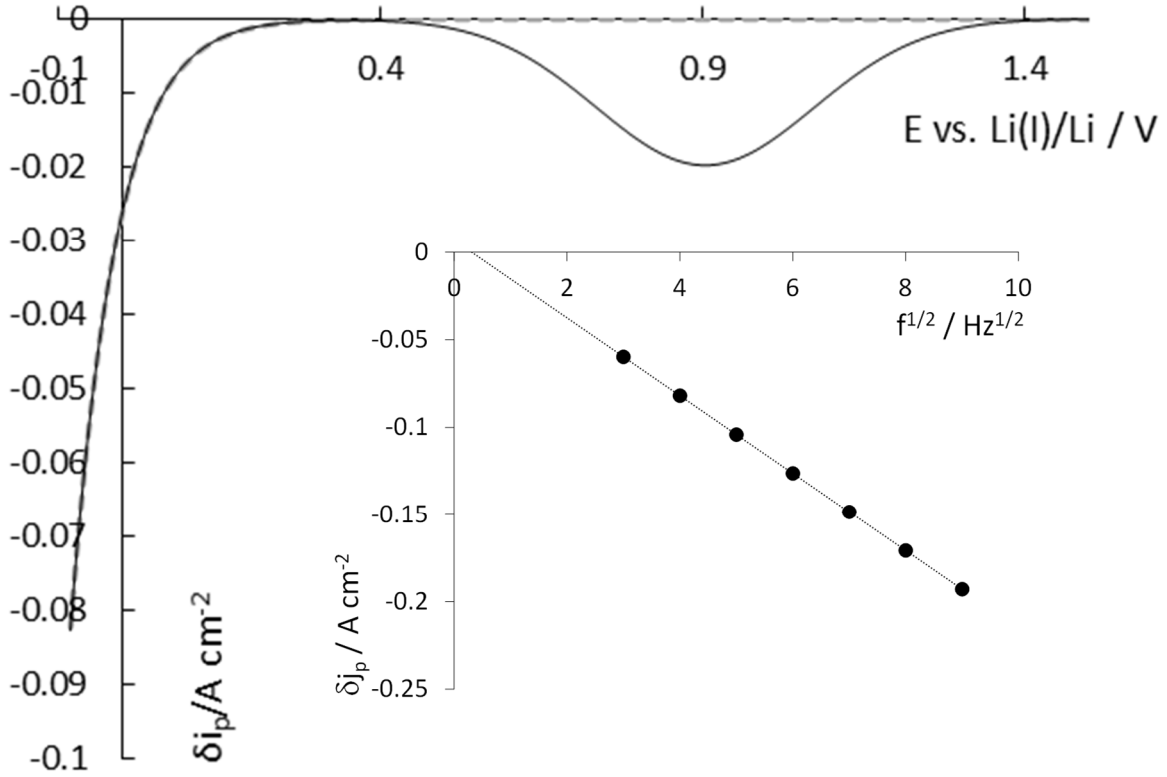

Figure 3b

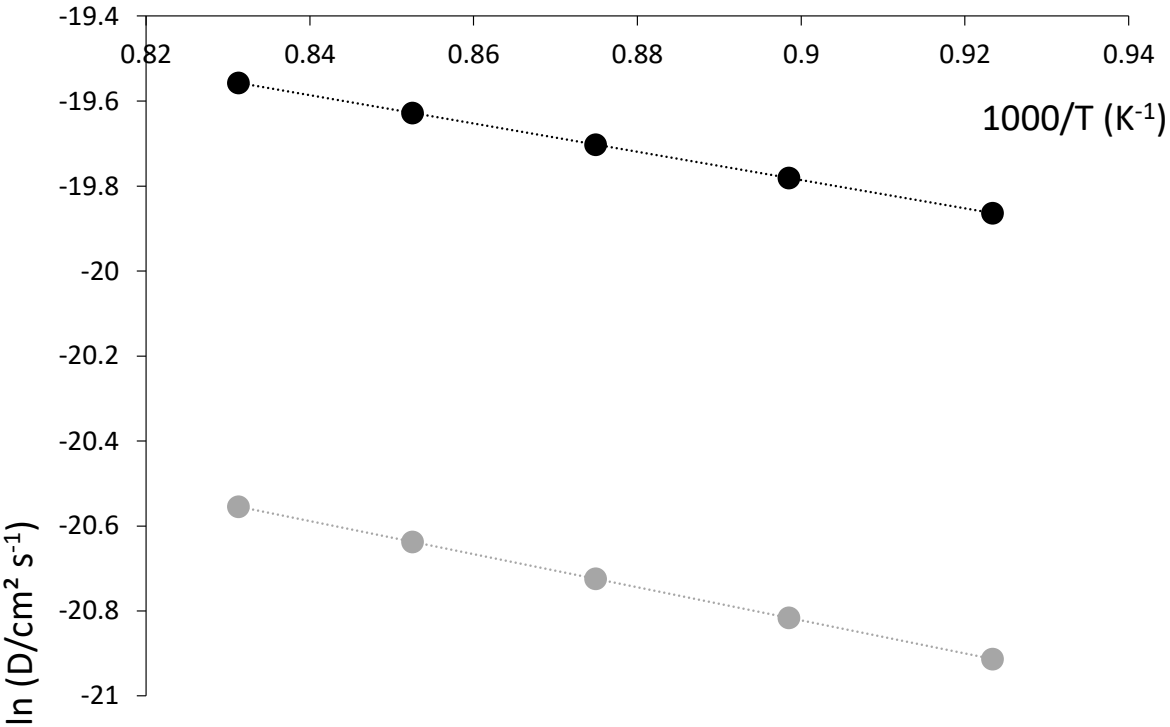

Figure 4

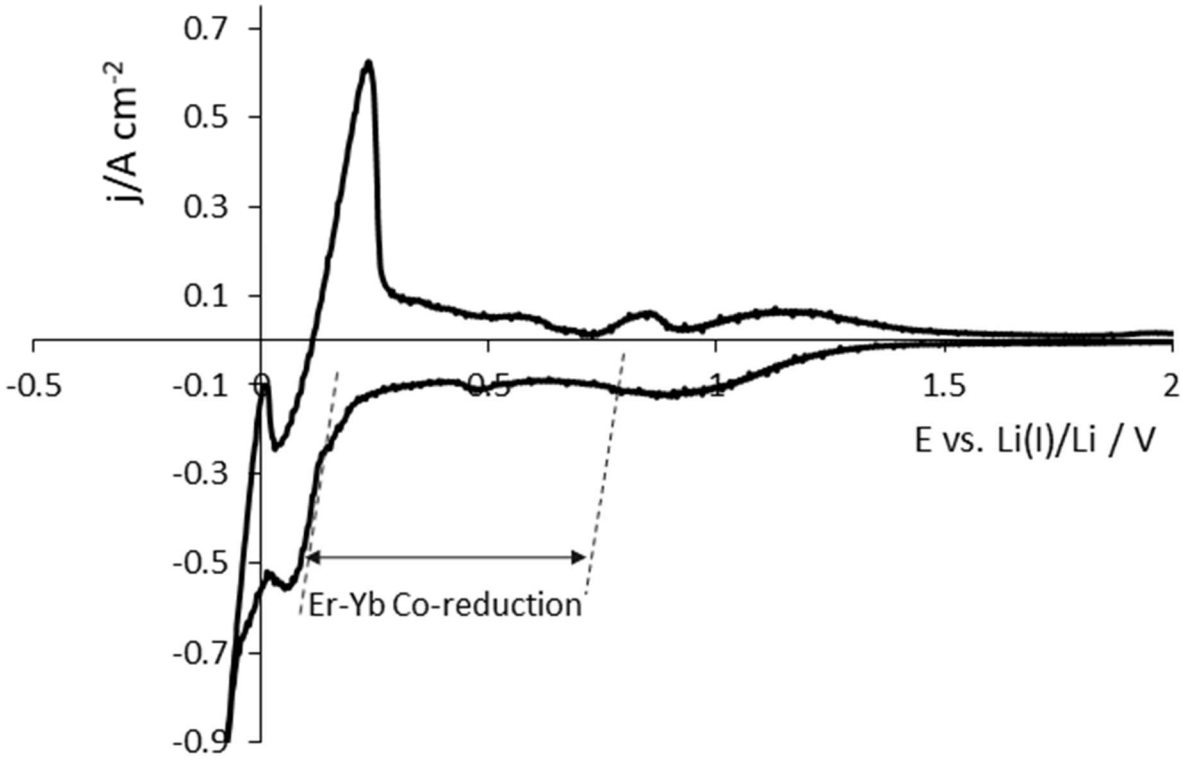

Figure 5a

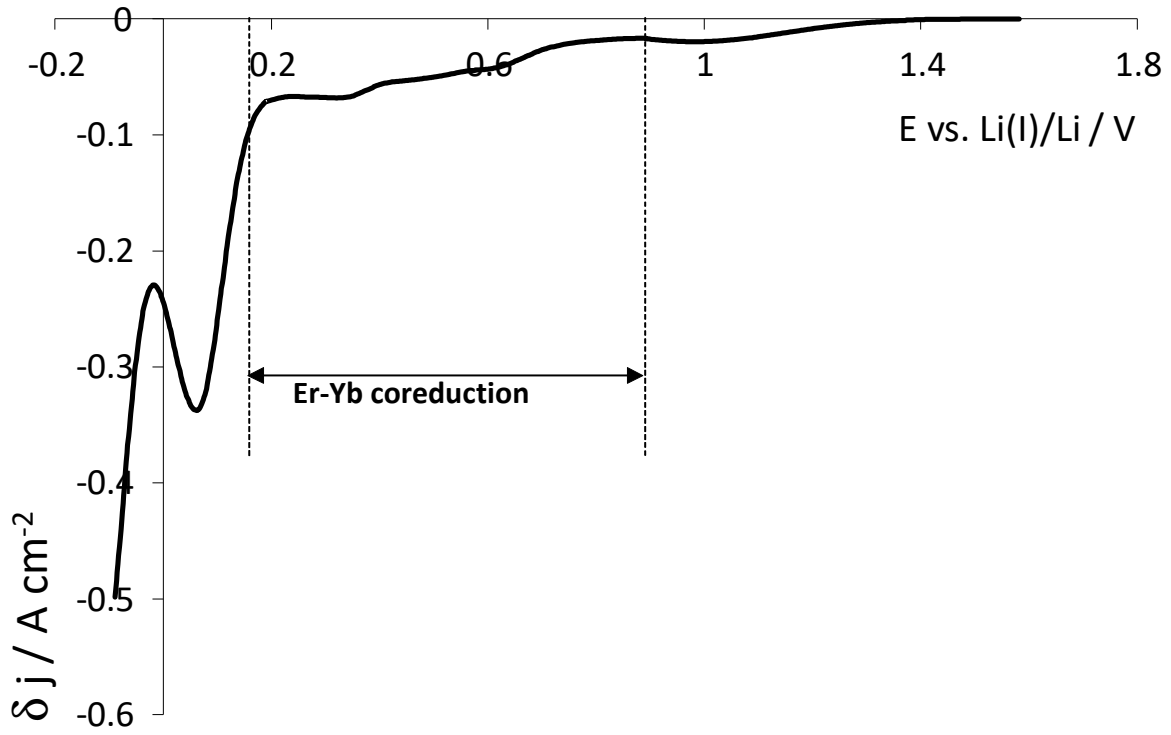

Figure 5b

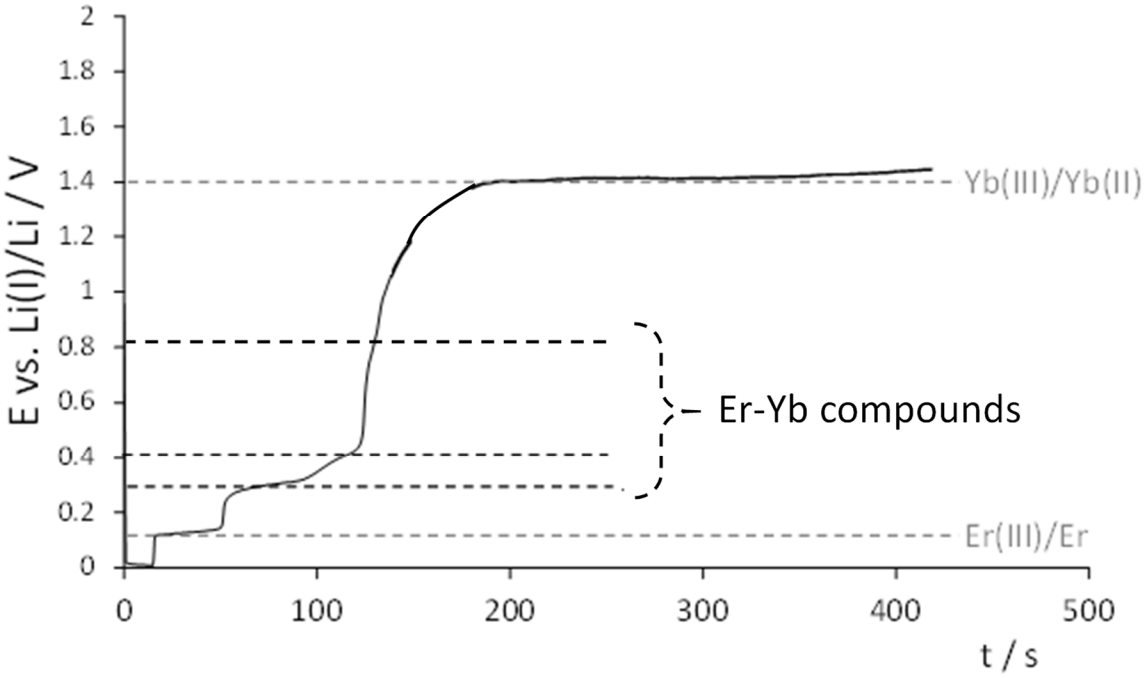

Figure 6

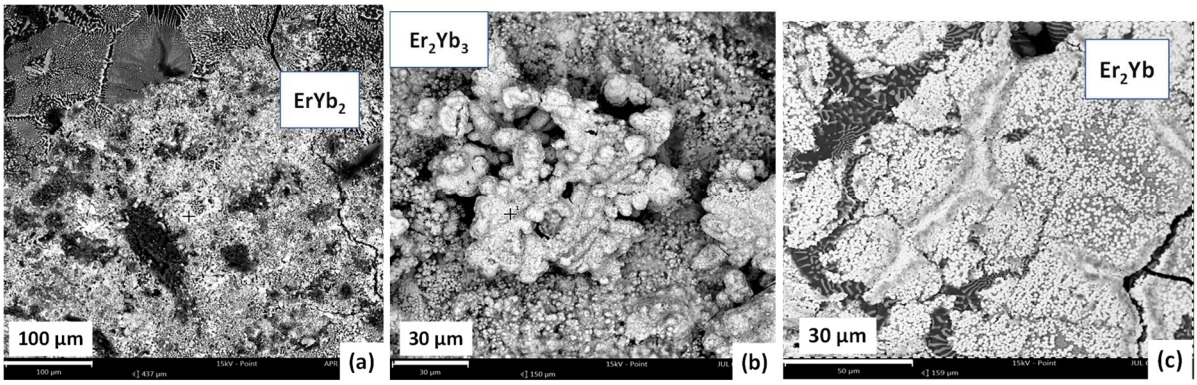

Figures 7a, b and c

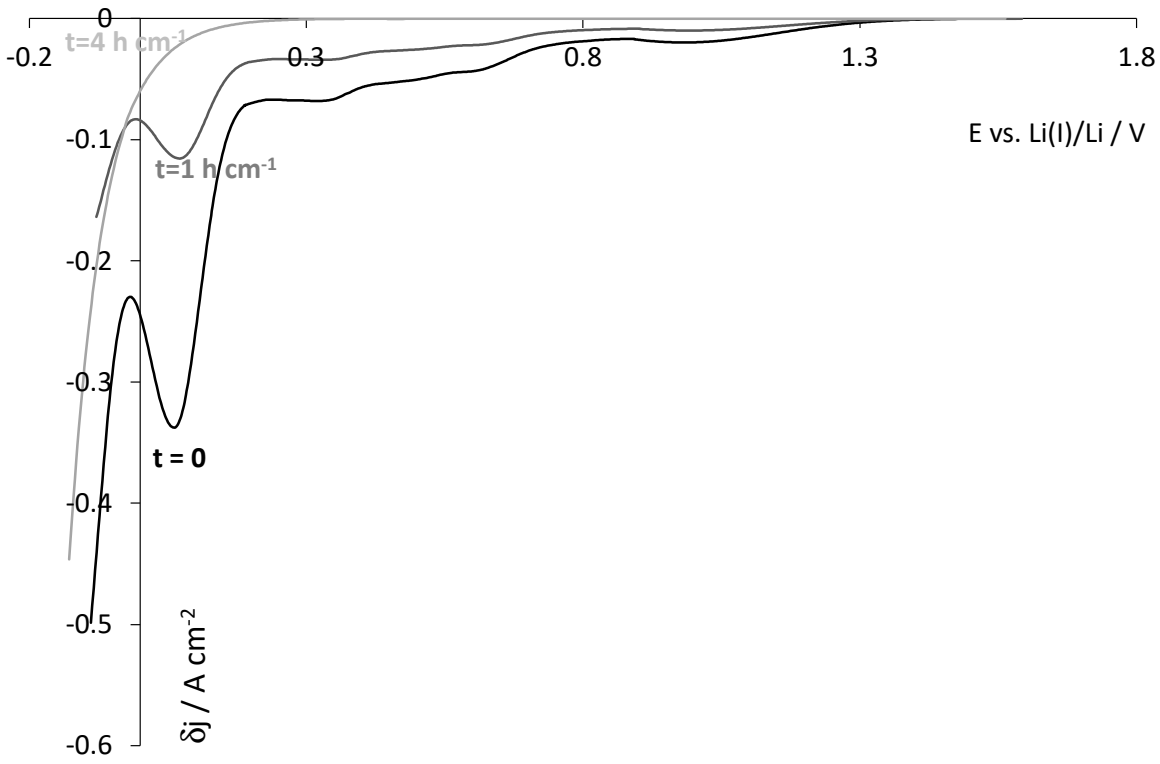

Figure 8

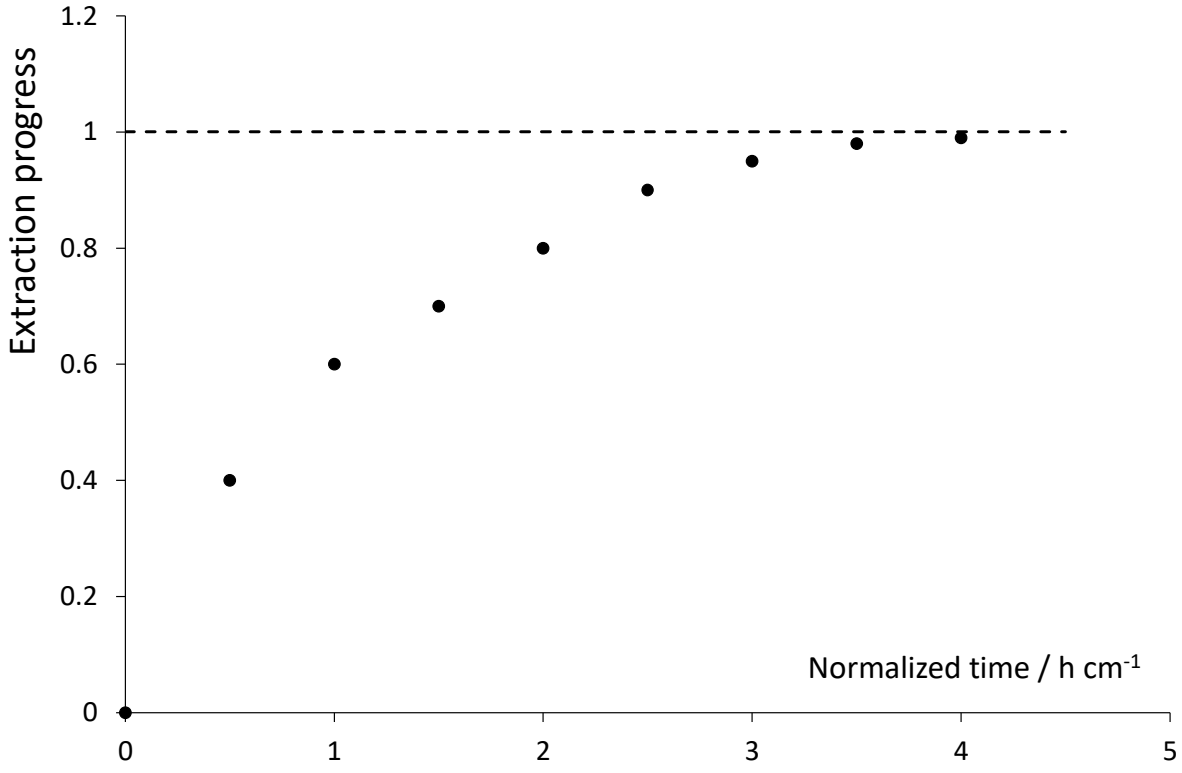

Figure 9

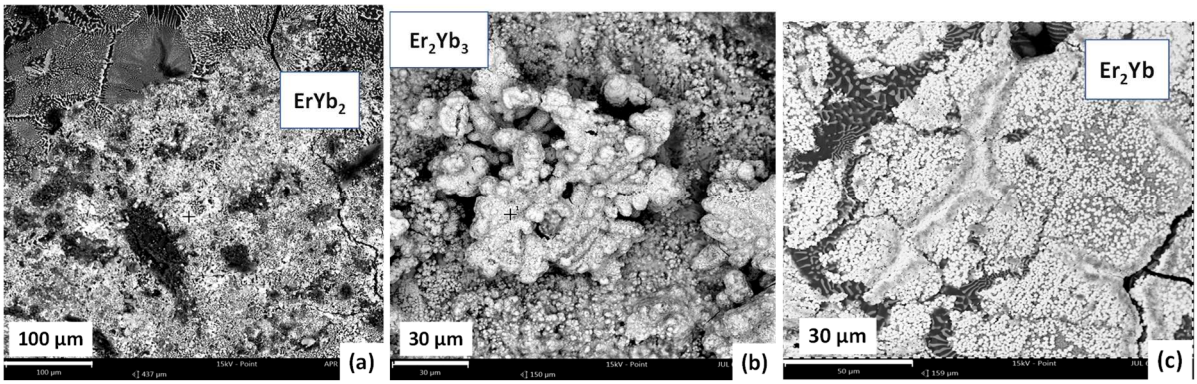

SEM micrographs of Mo electrodes after electrolysis at (a) 0.8 V vs. Li(I)/Li; (b) 0.4 V vs. Li(I)/Li and (c) 0.3 V vs. Li(I)/Li during 1800 s at 840°C.